

Inclusive Gluon Production in Pion-Proton Collisions and the Principle Maximum Conformality Renormalization Scale

A. I. Ahmadov^{1,2} ^{*}, C. Aydin^{1,3} [†], and O. Uzun¹ [‡]

¹ *Department of Physics, Karadeniz Technical University, 61080, Trabzon, Turkey*

² *Department of Theoretical Physics, Baku State University,*

Z. Khalilov st. 23, AZ-1148, Baku, Azerbaijan

³ *Department of Physics, University of Surrey,*

Guildford Surrey GU2 7XH, United Kingdom

(Dated: September 10, 2018)

Abstract

The contribution of the higher-twist mechanism to the large- p_T inclusive gluon production cross section in πp collisions is calculated in case of the principle of maximum conformality and Brodsky-Lepage-Mackenzie approaches in the dependence of the pion distribution amplitudes. The higher-twist cross sections obtained in the framework of the principle of maximum conformality and Brodsky-Lepage-Mackenzie approaches, and compared and analyzed in relation to the leading-twist cross sections and each other.

PACS numbers: 12.38.-t, 13.60.Le, 14.40.Aq, 13.87.Fh

Keywords: higher-twist, pion distribution amplitude, renormalization scale

^{*} E-mail: ahmadovazar@yahoo.com

[†] E-mail: coskun@ktu.edu.tr

[‡] E-mail: oguzhan_deu@hotmail.com

I. INTRODUCTION

It is well known that Quantum chromodynamics(QCD) is the fundamental theory of the strong interactions. Many researchers study QCD to describe the structure and dynamics of hadrons at the amplitude level. The hadronic distribution amplitude in terms of internal structure degrees of freedoms is important in QCD process predictions.

One of the basic problems is choosing the renormalization scale in running coupling constant $\alpha_s(Q^2)$. It is already stated in Ref. [1] that in perturbative QCD (pQCD) calculations, the argument of the running coupling constant in both the renormalization and factorization scale Q^2 should be taken equal as to the square of the momentum transfer of a hard gluon in a corresponding Feynman diagram. However, in this definition infrared singularity is removed in $\alpha_s(Q^2)$. Optimal approaches for solution of this problem can be found with the Brodsky-Lepage-Mackenzie (BLM) [1] and the Principle of Maximum Conformality (PMC) [2] methods.

In the perturbative QCD, the physical information of the inclusive gluon production is obtained efficiently; therefore, it can be directly compared to the experimental data.

Using the frozen and running coupling constant approaches the higher twist effects were already calculated by many authors [3–15].

The calculation and analysis of the higher-twist effects on the dependence of the pion distribution amplitude in inclusive gluon production at πp collision within PMC and BLM approaches are important research problem. In this work we computed the contribution of the higher-twist effects to an inclusive gluon production cross section by using various pion distribution amplitudes from holographic and perturbative QCD. We have also estimated and performed comparisons of the leading and the higher-twist contributions.

The mechanism for choosing renormalization scale is provided in Sec. II. Some formulas for the higher-twist and leading-twist cross sections are presented in Sec. III, and the numerical results for the cross section and discussion of the dependence of the cross section on the pion distribution amplitudes are provided in Sec. IV. Finally, our conclusions and the highlights of the study are listed in Sec. V.

II. CHOOSING THE RENORMALIZATION SCALE USING THE PRINCIPLE OF MAXIMUM CONFORMALITY

In principle, all measurable quantities in QCD should be invariant under any choice of renormalization scale and scheme. It is clear that the use of different scales and schemes may lead to different theoretical predictions. Taking into account this fact the constructive mathematical apparatus for defining QCD is a choice of the renormalization scale which makes scheme independent results at all fixed order in running coupling constant α_s .

The main idea of PMC/BLM, proposed and being developed by Brodsky *et al.* [2, 16–20], is that after proper procedures, all nonconformal β_i terms in the perturbative expansion are collected into the running coupling so that the remaining terms in the perturbative series are identical to those of a conformal theory, namely the corresponding theory with $\beta_i = 0$. Then the QCD predictions from PMC/BLM are independent of renormalization scheme. It has been found that PMC/BLM satisfies all self-consistent conditions [21]. As analyzed in Ref. [20], after PMC/BLM scale setting, the divergent renormalon series ($n! \beta_i^n \alpha_s^n$) does not appear in the conformal series.

Usually in QCD calculations, one chooses the renormalization scale μ^2 equal to $Q^2, p_T^2, \dots, p_T^2/2$, where Q^2 is a typical momentum transfer in the process obtained directly from Feynman diagram and p_T^2 is the squared transfer momentum of the observed particle. This approach has a problem, predicting QCD cross sections becoming negative at next-to-leading order [2, 22].

The renormalization scale in QED, for example in the modified minimal subtraction (\overline{MS}) scheme, has the form [2],

$$\mu_{\overline{MS}}^2 = Q^2 e^{-5/3} \quad (2.1)$$

if $Q^2 = -q^2$ is spacelike.

Therefore, we can choose

$$\alpha_{\overline{MS}}(q^2 e^{-5/3}) = \alpha_{GM-L}(q^2). \quad (2.2)$$

Such an analogy of renormalization scales between the \overline{MS} and Gell-Mann-Low schemes leads to the displacement of these schemes with $e^{-5/3}$ factor. It was chosen to determine and provide the minimal dimensional regularization scheme [2, 23].

Thus the PMC scale for the calculation differential cross section in the \overline{MS} scheme is given simply by the \overline{MS} scheme displacement of the gluon virtuality as $\mu_{PMC}^2 = e^{-5/3}Q^2$.

The PMC method is a general approach to set the renormalization scale in QCD, including purely gluonic processes. It is scheme independent and avoids the renormalon growth due to the absence of the β function terms in the perturbative expansion. Since the β -function in QCD is gauge invariant in any correct renormalization scheme, the resulting conformal series is also gauge invariant. Thus, the PMC is a gauge-invariant procedure.

For the calculation of QCD processes various schemes are used, such as minimal subtraction (MS), modified minimal subtraction \overline{MS} , momentum subtraction (MOM) or the BLM scheme. In the higher-twist processes, one of the main problem is choosing renormalization scale. In this paper, for the fixing renormalization scale, PMC method is used and compared with the BLM method.

III. HIGHER-TWIST AND LEADING-TWIST CONTRIBUTIONS TO INCLUSIVE GLUON PRODUCTION

The higher-twist Feynman diagrams for the inclusive gluon production in the pion-proton collision $\pi p \rightarrow gX$ are shown in Fig.1. The amplitude for this subprocess is found by means of the Brodsky-Lepage formula [24]

$$M(\hat{s}, \hat{t}) = \int_0^1 dx_1 \int_0^1 dx_2 \delta(1 - x_1 - x_2) \Phi_M(x_1, x_2, Q^2) T_H(\hat{s}, \hat{t}; x_1, x_2) \quad (3.1)$$

where T_H is the sum of the graphs contributing to the hard-scattering part of the subprocess. For the higher-twist, the subprocess $\pi q_p \rightarrow gq$ is taken, which contributes to $\pi p \rightarrow gX$, where q_p is a constituent of the initial proton target. As seen from Fig.1, processes $\pi^+ p \rightarrow gX$ and $\pi^- p \rightarrow gX$ arise from subprocesses as $\pi^+ d_p \rightarrow gu$ and $\pi^- u_p \rightarrow gd$, respectively.

We calculate the inclusive gluon production higher-twist cross section for various pion distribution amplitudes. Therefore, the higher-twist subprocess $\pi p \rightarrow gX$ is incorporated into the full inclusive cross section.

The production of the hadronic gluon or jets in the large transverse momentum is available at the high energy, especially at the Large Hadron Collider. Hadronic gluon as final are a product of the hard-scattering processes, before hadronization. In the final state this hadronic gluon or jets are fragmented or converted to hadron. Dynamical properties of

the jet is close to the parent parton, which carried one of the part four momentum of parent parton. Therefore, to get closer to the underlying parton level kinematics the gluon production process should be studied [25].

We can write the higher-twist cross section as

$$E \frac{d\sigma}{d^3 p}(\pi p \rightarrow gX) = \int_0^1 dx \delta(\hat{s} + \hat{t} + \hat{u}) \hat{s} G_{q/p}(x, Q^2) \frac{1}{\pi} \frac{d\sigma}{d\hat{t}}(\pi q_p \rightarrow gq), \quad (3.2)$$

where $G_{q/p}(x, Q^2)$ is the quark distribution function inside a proton.

The Mandelstam invariant variables for higher-twist subprocess $\pi q_p \rightarrow gq$ we can write in the form:

$$\hat{s} = (p_1 + p_g)^2 = (p_2 + p_\pi)^2, \quad \hat{t} = (p_g - p_\pi)^2, \quad \hat{u} = (p_1 - p_\pi)^2. \quad (3.3)$$

and from [26]

$$\frac{d\sigma}{d\hat{t}}(\hat{s}, \hat{t}, \hat{u}) = \frac{256\pi^2}{81\hat{s}^2} [D(\hat{s}, \hat{u})]^2 \left(-\frac{\hat{t}}{\hat{s}^2} - \frac{\hat{t}}{\hat{u}^2} \right), \quad (3.4)$$

where

$$D(\hat{s}, \hat{u}) = \int_0^1 dx \alpha_s^{3/2}(Q_1^2) \left[\frac{\Phi_\pi(x, Q_1^2)}{x(1-x)} \right] + \int_0^1 dx \alpha_s^{3/2}(Q_2^2) \left[\frac{\Phi_\pi(x, Q_2^2)}{x(1-x)} \right], \quad (3.5)$$

$Q_1^2 = (1-x)\hat{s}$ and $Q_2^2 = -x\hat{u}$ represent the momentum square of the hard gluon in Fig.1. So, in the BLM approach renormalization scales are $\mu_1^{BLM} = Q_1$ and $\mu_2^{BLM} = Q_2$, but in the PMC approach they are $\mu_1^{PMC} = Q_1 e^{-5/6}$ and $\mu_2^{PMC} = Q_2 e^{-5/6}$.

There are many forms of pion distribution amplitude available in the literature. In our numerical calculations, we used several choices, such as the asymptotic distribution amplitude derived in pQCD evalution [27], the Vega-Schmidt-Branz-Gutsche-Lyubovitskij (VSBGL) distribution amplitude [28], distribution amplitudes predicted by AdS/CFT [29, 30], and the Chernyak-Zhitnitsky(CZ) [31], the Bakulev-Mikhailov-Stefanis (BMS) [32] and twist-three distribution amplitudes (HW) [33]:

$$\Phi_{asy}(x) = \sqrt{3} f_\pi x(1-x), \quad (3.6)$$

$$\Phi_{VSBGL}^{hol}(x) = \frac{A_1 k_1}{2\pi} \sqrt{x(1-x)} \exp \left(-\frac{m^2}{2k_1^2 x(1-x)} \right), \quad (3.7)$$

$$\Phi^{hol}(x) = \frac{4}{\sqrt{3}\pi} f_\pi \sqrt{x(1-x)}, \quad (3.8)$$

$$\Phi_{CZ}(x, \mu_0^2) = \Phi_{asy}(x) \left[C_0^{3/2} (2x-1) + \frac{2}{3} C_2^{3/2} (2x-1) \right], \quad (3.9)$$

$$\Phi_{BMS}(x, \mu_0^2) = \Phi_{asy}(x) \left[C_0^{3/2}(2x-1) + 0.20C_2^{3/2}(2x-1) - 0.14C_4^{3/2}(2x-1) \right], \quad (3.10)$$

$$\Phi_{HW}(x) = \frac{A_p \beta^2}{2\pi^2} \left[1 + B_p C_2^{1/2}(2x-1) + C_p C_4^{1/2}(2x-1) \right] \exp \left(-\frac{m^2}{8\beta^2 x(x-1)} \right), \quad (3.11)$$

$C_n^\lambda(2x-1)$ are Gegenbauer polynomials with the recurrence relation

$$nC_n^{(\lambda)}(\xi) = 2(n+\lambda-1)\xi C_{n-1}^{(\lambda)}(\xi) - (n+2\lambda-2)C_{n-2}^{(\lambda)}(\xi). \quad (3.12)$$

The pion distribution amplitude can be expanded as

$$\Phi_\pi(x, Q^2) = \Phi_{asy}(x) \left[1 + \sum_{n=2,4..}^{\infty} a_n(Q^2) C_n^{3/2}(2x-1) \right]. \quad (3.13)$$

Finally, differential cross section for the process $\pi p \rightarrow gX$ is written as [25]

$$E \frac{d\sigma}{d^3 p}(\pi p \rightarrow gX) = \frac{s}{s+u} x G_{q/p}(x, Q^2) \frac{256\pi}{81\hat{s}^2} [D(\hat{s}, \hat{u})]^2 \left(-\frac{\hat{t}}{\hat{s}^2} - \frac{\hat{t}}{\hat{u}^2} \right). \quad (3.14)$$

It should be noted that, as seen from Eq.(3.4) and Eq.(3.14), the higher-twist cross section is linear with respect to \hat{t} , so the cross section vanishes if the scattering angle between the final gluon and incident pion is approximately equal to zero, $\theta = 0$. Also, as seen from Eq.(3.4), the higher-twist cross section proportional to \hat{s}^{-3} , which shows that higher-twist contributions to the $\pi p \rightarrow gX$ cross section have the form of $p_T^{-6} f(x_F, x_T)$.

The difficulty comes in extracting the higher-twist corrections to the inclusive gluon production cross section. One can also consider the comparison of higher-twist corrections with leading-twist contributions. For the leading-twist subprocess in the inclusive gluon production, we take $q\bar{q} \rightarrow g\gamma$ as a subprocess of the quark-antiquark annihilation. The differential cross section for subprocess $q\bar{q} \rightarrow g\gamma$ is

$$\frac{d\sigma}{d\hat{t}}(q\bar{q} \rightarrow g\gamma) = \frac{8}{9} \pi \alpha_E \alpha_s(Q^2) \frac{e_q^2}{\hat{s}^2} \left(\frac{\hat{t}}{\hat{u}} + \frac{\hat{u}}{\hat{t}} \right). \quad (3.15)$$

As seen from Eq.(3.15), the leading-twist is proportional to p_T^{-4} .

The leading-twist cross section for production of inclusive gluon is [34]

$$\Sigma_M^{LT} \equiv E \frac{d\sigma}{d^3 p}(\pi p \rightarrow gX) = \int_0^1 dx_1 \int_0^1 dx_2 \delta(\hat{s} + \hat{t} + \hat{u}) G_{\bar{q}/M}(x_1, Q_1^2) G_{q/p}(x_2, Q_2^2) \frac{\hat{s}}{\pi} \frac{d\sigma}{d\hat{t}}(q\bar{q} \rightarrow g\gamma), \quad (3.16)$$

where

$$\hat{s} = x_1 x_2 s, \quad \hat{t} = x_1 t, \quad \hat{u} = x_2 u.$$

The leading-twist contribution to the large- p_T gluon production cross section in the process $\pi p \rightarrow gX$ is

$$\Sigma_M^{LT} \equiv E \frac{d\sigma}{d^3 p}(\pi p \rightarrow gX) = \int_0^1 dx_1 \frac{1}{x_1 s + u} G_{\bar{q}/M}(x_1, Q_1^2) G_{q/p}(1 - x_1, Q_2^2) \frac{\hat{s}}{\pi} \frac{d\sigma}{dt}(q\bar{q} \rightarrow g\gamma). \quad (3.17)$$

We denote higher-twist cross section calculated with the PMC and BLM approaches by $(\Sigma_g^{HT})_{PMC}$ and $(\Sigma_g^{HT})_{BLM}$, respectively.

IV. NUMERICAL RESULTS AND DISCUSSION

We will discuss for the higher-twist contribution in the process of inclusive gluon production in πp collisions. In the numerical calculations for the fixing renormalization scale, we applied the PMC and BLM approaches. For $\pi^+ p \rightarrow gX$ and $\pi^- p \rightarrow gX$ processes, we take $\pi^+ d_p \rightarrow gu$, and $\pi^- u_p \rightarrow gd$ as respective subprocesses.

For the dominant leading-twist subprocess for the gluon production, the quark-antiquark annihilation $q\bar{q} \rightarrow \gamma g$ is taken. For the quark distribution functions inside the pion and proton, we used expressions given in Refs. [35, 36], respectively. We present our results for $\sqrt{s} = 62.4 \text{ GeV}$, since this value is planned for a future Fermilab experiment.

Obtained results are visualized in Figs. 2-15. In all figures we represent the choice of pion distribution amplitudes Eqs.(3.6)-(3.11) by different line types: $\Phi_{asy}(x)$ as solid black line, $\Phi^{hol}(x)$ as dashed red line, $\Phi_{VSBGL}^{hol}(x)$ as dotted blue line, $\Phi_{CZ}(x, Q^2)$ as dash-dot magenta line, $\Phi_{BMS}(x, Q^2)$ as dash-double dot olive line, and $\Phi_{HW}(x, Q^2)$ as short dash navy line.

First, we compare higher-twist cross sections obtained with the PMC and BLM approaches. In Fig. 2 and 3 the dependence of higher-twist cross sections $(\Sigma_g^{HT})_{PMC}$ and $(\Sigma_g^{HT})_{BLM}$ are shown as a function of the gluon transverse momentum p_T for various choices the pion distribution amplitudes at $y = 0$. It can be observed from those figures that the higher-twist cross section is monotonically decreasing with the increase of the transverse momentum of the gluon. In the region $2 \text{ GeV}/c < p_T < 30 \text{ GeV}/c$ the $(\Sigma_g^{HT})_{PMC}$ cross sections of the process $\pi^+ p \rightarrow \gamma X$ decrease in the range between $1.72 \cdot 10^{-2} \mu\text{b}/\text{GeV}^2$ to $2.13 \cdot 10^{-13} \mu\text{b}/\text{GeV}^2$.

In Fig. 4, the dependence of the ratio $(\Sigma_g^{HT})_{PMC}/(\Sigma_g^{HT})_{BLM}$ is displayed for the process $\pi^+ p \rightarrow gX$ as a function of p_T for all pion distribution amplitudes. We see that in the region $5 \text{ GeV}/c < p_T < 30 \text{ GeV}/c$, the PMC cross sections for all distribution amplitudes

are enhanced by about factor of 2 relative to corresponding BLM cross sections. We also see that the ratio $(\Sigma_g^{HT})_{PMC}/(\Sigma_g^{HT})_{BLM}$ for $\Phi_{HW}(x, Q^2)$ distribution amplitude is identically equivalent to ratios for Φ_{asy} , $\Phi^{hol}(x)$ and $\Phi_{VSBGL}^{hol}(x)$ distribution amplitudes.

In Fig. 5 and 6 the dependence of higher-twist cross sections $(\Sigma_g^{HT})_{PMC}$ and $(\Sigma_g^{HT})_{BLM}$ on the process $\pi^-p \rightarrow gX$ is displayed as a function of the gluon transverse momentum p_T for the pion distribution amplitudes presented in Eqs.(3.6)-(3.11) at $y = 0$. As is seen in Fig. 5, in the region $2 \text{ GeV}/c < p_T < 30 \text{ GeV}/c$, PMC cross section for the $\Phi_{HW}(x, Q^2)$ distribution amplitude is enhanced by about 2 orders of magnitude relative to the all other distribution amplitudes. The similar dependence of the BLM cross sections is shown in Fig. 6.

The dependence of the ratios $(\Sigma_g^{HT})_{PMC}/(\Sigma_g^{HT})_{BLM}$, $(\Sigma_g^{HT})_{PMC}/(\Sigma_g^{LT})$ in the process $\pi^-p \rightarrow gX$ as a function of p_T for the various pion distribution amplitudes is displayed in Figs. 7-9. One of the interesting results is that ratios $(\Sigma_g^{HT})_{PMC}/(\Sigma_g^{HT})_{BLM}$ for processes $\pi^+p \rightarrow gX$ and $\pi^-p \rightarrow gX$ are identically equivalent. In Figs. 8-9 we show ratios $(\Sigma_g^{HT})_{PMC}/(\Sigma_g^{LT})$ for processes $\pi^\pm p \rightarrow gX$ as a function of p_T . As is seen from these figures, in the region $2 \text{ GeV}/c < p_T < 22 \text{ GeV}/c$, leading-twist cross sections is enhanced by about 2 to 3 orders of magnitude relative to the PMC cross sections for all pion distribution amplitudes.

In Figs. 10-15, the dependence of higher-twist cross sections $(\Sigma_g^{HT})_{PMC}$, $(\Sigma_g^{HT})_{BLM}$, ratios $(\Sigma_g^{HT})_{PMC}/(\Sigma_g^{HT})_{BLM}$, $(\Sigma_g^{HT})_{PMC}/(\Sigma_g^{LT})$ on processes $\pi^\pm p \rightarrow gX$ is shown as a function of the rapidity y of the gluon at the transverse momentum of the gluon $p_T = 4.9 \text{ GeV}/c$. It is seen in Figs. 10-12 that the cross sections in the PMC and BLM approaches, and the ratio for all distribution amplitudes of pion, have a maximum approximately at the point $y = -2$. Notice that the maximum for the CZ amplitude in PMC is more pronounced: due to PMC the cross section for the $\Phi_{HW}(x, Q^2)$ distribution amplitude is enhanced by about 2 to 3 orders of magnitude relative to all other distribution amplitudes. The same dependence for the BLM cross sections is seen in Fig. 11. In Fig. 12 we show the ratio PMC/BLM cross sections as a function of the rapidity of gluons as $\pi^+p \rightarrow gX$. We see that the ratios for all distribution amplitudes are close to each other. Similar results for $\pi^-p \rightarrow gX$ are displayed in Fig. 13-15. We think that this feature of the comparison between PMC and BLM cross sections may help to explain theoretical interpretations with future experimental data for the inclusive gluon production cross section in the pion-proton collisions. Higher-twist cross

section obtained in our study should be observable at hadron collider.

We can see in Figs. 2, 3, 5, 6, 10, 11, 13, and 14 that cross sections for twist-3 distribution amplitudes calculated within PMC/BLM schemes are significantly different from the others. This behaviour can be explained by the following: first, in the twist-3 distribution amplitude defined in Eq.(3.11), the usual helicity components ($\lambda_1 + \lambda_2 = 0$) have been taken into account. However, the higher helicity components ($\lambda_1 + \lambda_2 = \pm 1$) that come from the spin-space Wigner rotation have not been considered. Second, in the twist-3 distribution amplitude construction, the contribution of the intrinsic quark propagator k_T is also included. Directly we can obtain, that the quark propagator, gives essential contribution for the twist-3 distribution amplitude, depending on the transverse momentum [33].

As one can see from the figures, there is a large difference between the cross sections calculated by PMC and BLM schemes. Main reasons for this are the following: as we know, the PMC scheme is defined in the form $(\mu_1^2)^{PMC} = (1-x)\hat{s}e^{-5/3}$ and $(\mu_2^2)^{PMC} = -x\hat{u}e^{-5/3}$, but the BLM scale in the form $(\mu_1^2)^{BLM} = (1-x)\hat{s}$ and $(\mu_2^2)^{PMC} = -x\hat{u}$. PMC and BLM schemes differ with the factor $e^{-5/3}$ and also take into account the running coupling constant proportional to $1/\ln(\mu^2/\Lambda^2)$. Therefore, cross sections calculated within the PMC scale are enhanced by cross section calculated within the BLM scale.

Notice that in Figs. 4, 7, 12, 15, the curves for ratio $(\Sigma_g^{HT})_{PMC}/(\Sigma_g^{HT})_{BLM}$ [as shown in figures: $asy(PMC)/asy(BLM)$, $hol(PMC)/hol(BLM)$, $VSBGL(PMC)/VSBGL(BLM)$, $HW(PMC)/HW(BLM)$] for distribution amplitudes $\Phi^{hol}(x)$, $\Phi_{asy}(x)$, $\Phi_{VSBGL}^{hol}(x)$ and $\Phi_{HW}(x, Q^2)$ cannot be resolved from each other because the corresponding cross section ratios are almost exactly equal.

V. CONCLUSIONS

In this paper, we have presented the inclusive gluon production cross section in the process πp collisions via higher-twist mechanisms within holographic and perturbative QCD. For calculation of the cross section, the renormalization scale in running coupling is applied within PMC and BLM approaches. The results obtained from the approaches PMC and BLM are different in some regions. These results also depend on the form of the pion distribution amplitudes. We compared BLM and PMC cross sections of the inclusive gluon production in the processes $\pi^- p \rightarrow gX$ and $\pi^+ p \rightarrow gX$. Our results show in both cases that

the inclusive gluon production cross section in the process $\pi^- p \rightarrow gX$ is suppressed over the inclusive gluon production cross section in the process $\pi^+ p \rightarrow gX$. Notice that the inclusive gluon production spectrum can be measured with large precision, so results obtained in this study will help further tests for hadron dynamics at large p_T . It is also observed that higher-twist cross sections are proportional to the third order of $\alpha_s(Q^2)$, but the leading-twist is linearly proportional to $\alpha_s(Q^2)$. Therefore, their ratio strongly depends of the $\alpha_s^2(Q^2)$.

Our calculation show that the higher helicity components in the higher-twist distribution amplitude make significant contributions to the cross section. We also note that the intrinsic transverse momentum of the distribution amplitude is very important for the cross section, and without including these effects one overestimates the results.

In our opinion higher-twist cross section obtained by PMC approach are approximately equivalent to the resummed cross section in the same process. Also, we hope that the PMC approach can be applied to a wide class of perturbatively calculable collider and other processes. Results obtaining within the PMC approach can improve the precision of tests of the Standard Model and enhance sensitivity to new physical phenomena.

Acknowledgments

The authors thank to Stanley J. Brodsky for useful discussions. We are also grateful to Dr. S.H.Aydin and A.Mustafayev for carefully reading the paper and providing useful comments. This work is supported by TUBITAK under grant number 2221(Turkey). A. I. A acknowledges hospitality the Department of Physics of Karadeniz Technical University during this work. The author C.A thanks to member of the Department of Physics at University of Surrey especially to Dr. Paul Stevenson giving opportunity to research in their institute.

- [1] S. J. Brodsky, G. L. Lepage, and P. B. Mackenzie, Phys. Rev. D **28**, 228 (1983).
- [2] S. J. Brodsky and L. Di Glustino, Phys. Rev. D **86**, 085026 (2012).
- [3] J. A. Bagger and J. F. Gunion, Phys. Rev. D **29**, 40 (1984).
- [4] A. Bagger and J. F. Gunion, Phys. Rev. D **25**, 2287 (1982).

[5] V. N. Baier and A. Grozin, Phys. Lett. **96B**, 181 (1980); S. Gupta, Phys. Rev. D**24**, 1169 (1981).

[6] F. S. Sadykhov and A. I. Akhmedov, Russ. Phys. J. **38**, 513 (1995).

[7] A. I. Ahmadov, I. Boztosun, R. Kh. Muradov, A. Soylu, and E. A. Dadashov, Int. J. Mod. Phys. E**15**, 1209 (2006).

[8] A. I. Ahmadov, I. Boztosun, A. Soylu, and E. A. Dadashov, Int. J. Mod. Phys. E**17**, 1041 (2008).

[9] A. I. Ahmadov, Coskun Aydin, Sh. M. Nagiyev, A. Hakan Yilmaz, and E. A. Dadashov, Phys. Rev. D**80**, 016003 (2009).

[10] A. I. Ahmadov, Coskun Aydin, E. A. Dadashov, and Sh. M. Nagiyev, Phys. Rev. D**81**, 054016 (2010).

[11] A. I. Ahmadov, R. M. Burjaliyev, Int. J. Mod. Phys. E**20**, 1243 (2011).

[12] A. I. Ahmadov, Sh. M. Nagiyev, and E. A. Dadashov, Int. J. Mod. Phys. E**21**, 1250014 (2012).

[13] A. I. Ahmadov, C. Aydin, and F. Keskin, Phys. Rev. D**85**, 034009 (2012).

[14] A. I. Ahmadov, C. Aydin, and F. Keskin, Ann. Phys. **327**, 1472 (2012).

[15] A. I. Ahmadov, C. Aydin, and O. Uzun, Phys. Rev. D**87**, 014006 (2013).

[16] S. J. Brodsky and Xing-Gang Wu, Phys. Rev. D**86**, 054018 (2012).

[17] S. J. Brodsky and Xing-Gang Wu, Phys. Rev. D**85**, 114040 (2012).

[18] S. J. Brodsky and Xing-Gang Wu, Phys. Rev. D**86**, 014021 (2012).

[19] S. J. Brodsky and Xing-Gang Wu, Phys. Rev. Lett. **109**, 042002 (2012).

[20] S. J. Brodsky and Xing-Gang Wu, Phys. Rev. D**85**, 034038 (2012).

[21] S.J. Brodsky, Report No. SLAC-PUB-6304, 1993; S.J. Brodsky and H.J. Lu, Report No. SLAC-PUB-6000.

[22] D. Maitre et al., PoS Sci., EPS-HEP(2009) 367.

[23] W. A. Bardeen, A. J. Buras, D. W. Duke, and T. Muta, Phys. Rev. D**18**, 3998 (1978).

[24] G. L. Lepage and S. J. Brodsky, Phys. Rev. D**22**, 2157 (1980).

[25] J.F. Owens, Rev. Modern Phys. **59**, 465 (1987).

[26] E. L. Berger and S. J. Brodsky, Phys. Rev. D**24**, 2428 (1981).

[27] G. P. Lepage and S. J. Brodsky, Phys. Lett. **87B**, 359 (1979).

[28] A. Vega, I. Schmidt, T. Branz, T. Gutsche, V. Lyubovitskij, Phys. Rev. D**80**, 055014 (2009).

- [29] S. J. Brodsky and G. F. de Teramond, Phys. Rev. D**77**, 056007 (2008).
- [30] S. J. Brodsky, Proc. Sci., LHC07 (2007) 002.
- [31] V. L. Chernyak and A. R. Zhitnitsky, Phys. Rep. **112**, 173 (1984).
- [32] A. P. Bakulev, S. V. Mikhailov and N. G. Stefanis, Phys. Lett. **B 578**, 91 (2004); A. P. Bakulev, S.V. Mikhailov, A.V. Pimikov, and N. G. Stefanis, Phys. Rev. D**86**, 031501 (2012).
- [33] T. Huang and X.-G. Wu, Phys. Rev. D**70**, 093013 (2004).
- [34] E. L. Berger, Phys. Rev. D**26**, 105 (1982).
- [35] S.-i Nam, Phys. Rev. D**86**, 074005 (2012).
- [36] A.D. Martin, W. J. Stirling, R.S. Thorne, G. Watt, Eur. Phys. J. C**63**, 189 (2009).

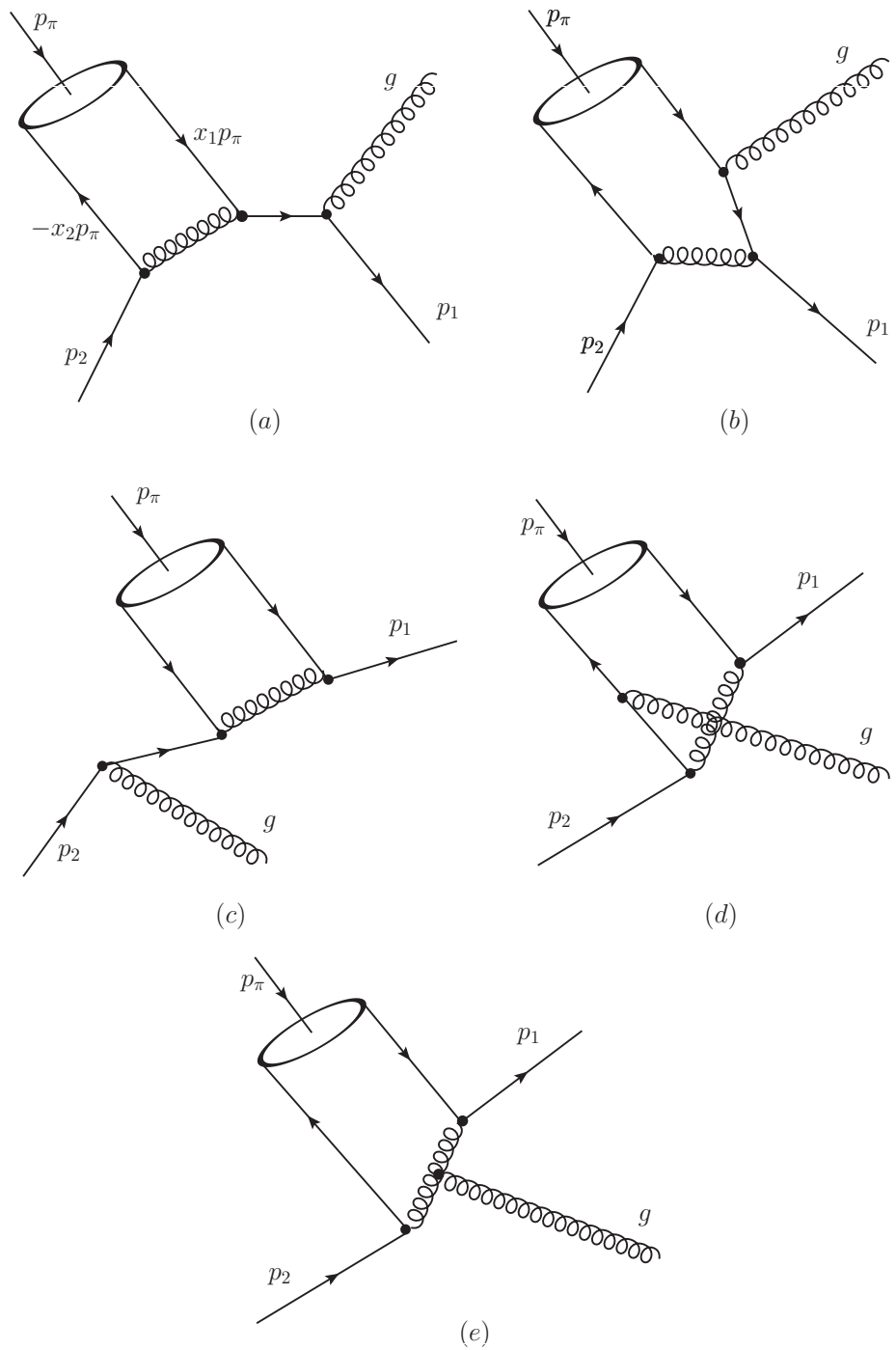


FIG. 1: Full set of QCD Feynman diagrams for higher-twist subprocess $\pi q \rightarrow g q$.

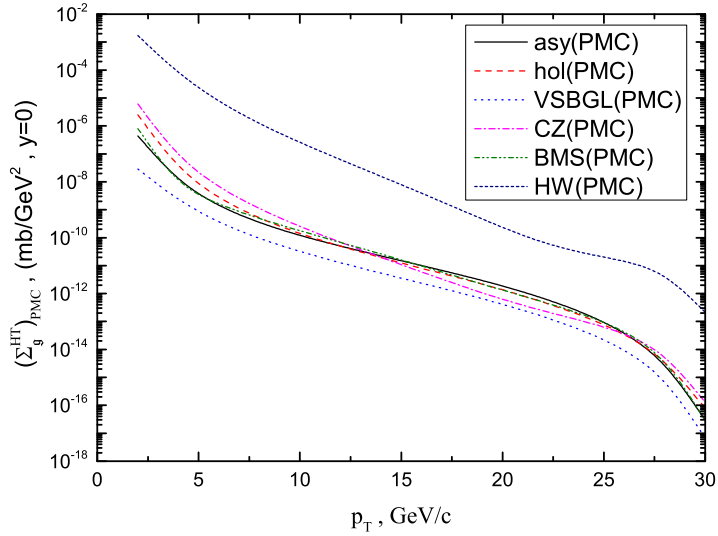


FIG. 2: Higher-twist $\pi^+ p \rightarrow gX$ inclusive gluon production cross section $(\Sigma_g^{HT})_{PMC}$ as a function of the p_T of the gluon at $\sqrt{s} = 62.4$ GeV.

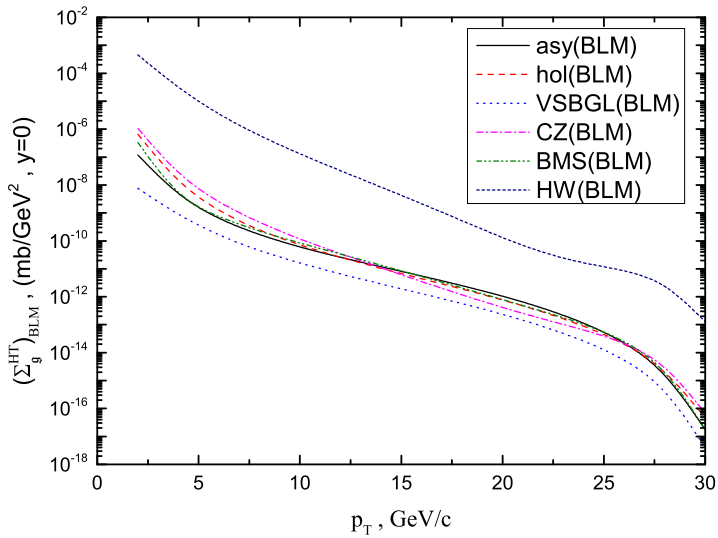


FIG. 3: Higher-twist $\pi^+ p \rightarrow gX$ inclusive gluon production cross section $(\Sigma_g^{HT})_{BLM}$ as a function of the p_T of the gluon at $\sqrt{s} = 62.4$ GeV.

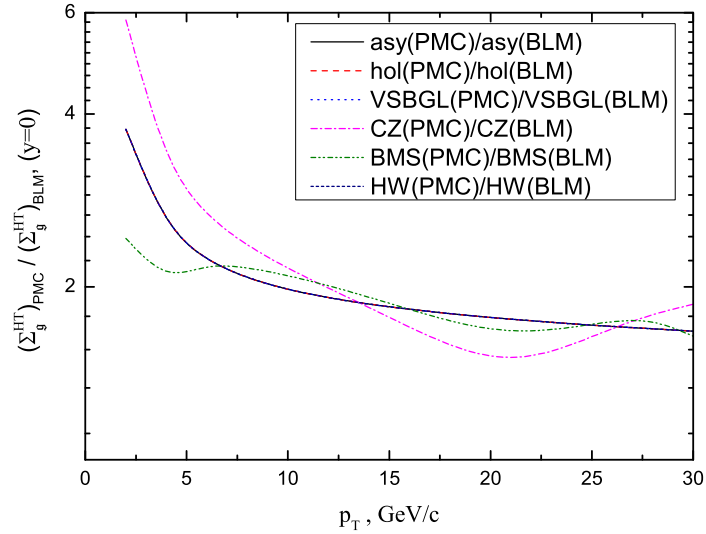


FIG. 4: Ratio $(\Sigma_g^{HT})_{PMC}/(\Sigma_g^{HT})_{BLM}$, in the process $\pi^+p \rightarrow gX$, where higher-twist contribution are calculated for the gluon rapidity $y = 0$ at $\sqrt{s} = 62.4 \text{ GeV}$ as a function of the p_T of the gluon. Notice that curves for asy(PMC)/asy(BLM), hol(PMC)/hol(BLM), VSBGL(PMC)/VSBGL(BLM), HW(PMC)/HW(BLM) pion distribution amplitudes completely overlap.

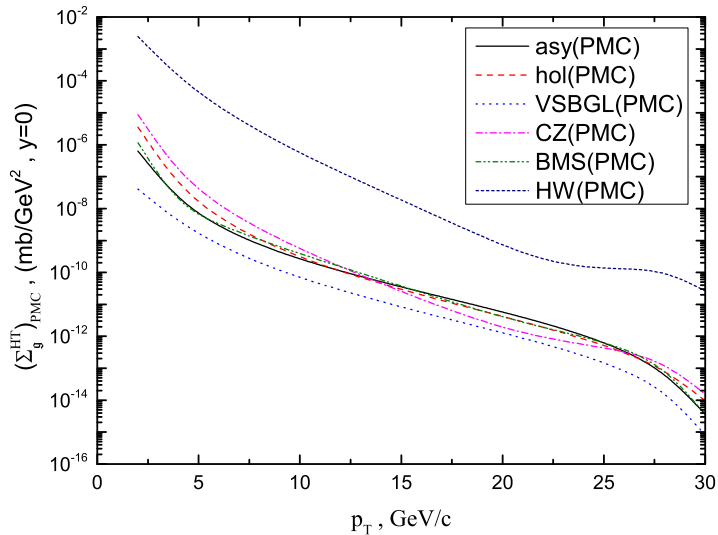


FIG. 5: Higher-twist $\pi^-p \rightarrow gX$ inclusive gluon production cross section $(\Sigma_g^{HT})_{PMC}$ as a function of the p_T of the gluon at $\sqrt{s} = 62.4 \text{ GeV}$.

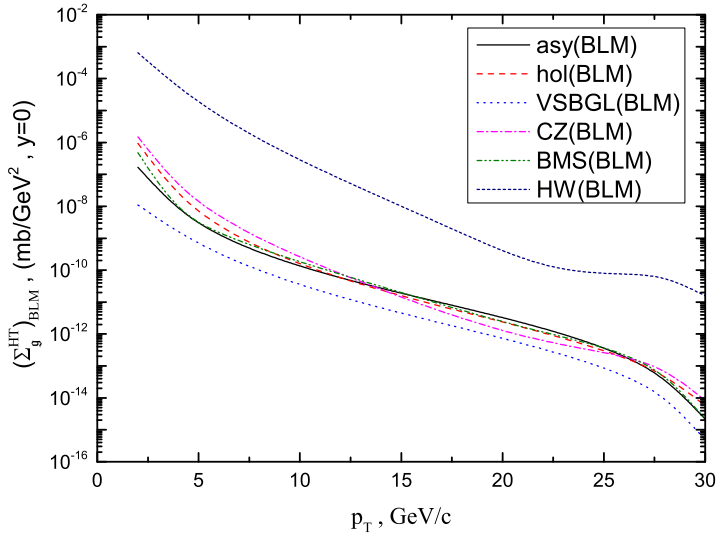


FIG. 6: Higher-twist $\pi^- p \rightarrow gX$ inclusive gluon production cross section $(\Sigma_g^{HT})_{BLM}$ as a function of the p_T of the gluon at $\sqrt{s} = 62.4$ GeV.

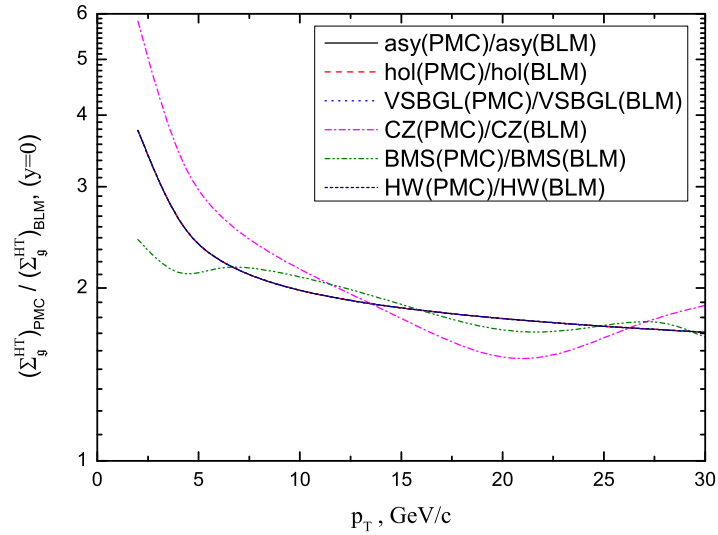


FIG. 7: Ratio $(\Sigma_g^{HT})_{PMC} / (\Sigma_g^{HT})_{BLM}$, in the process $\pi^- p \rightarrow gX$, where higher-twist contribution are calculated for the gluon rapidity $y = 0$ at $\sqrt{s} = 62.4$ GeV as a function of the p_T of the gluon. Notice that curves for asy(PMC)/asy(BLM), hol(PMC)/hol(BLM), VSBGL(PMC)/VSBGL(BLM), HW(PMC)/HW(BLM) pion distribution amplitudes completely overlap.

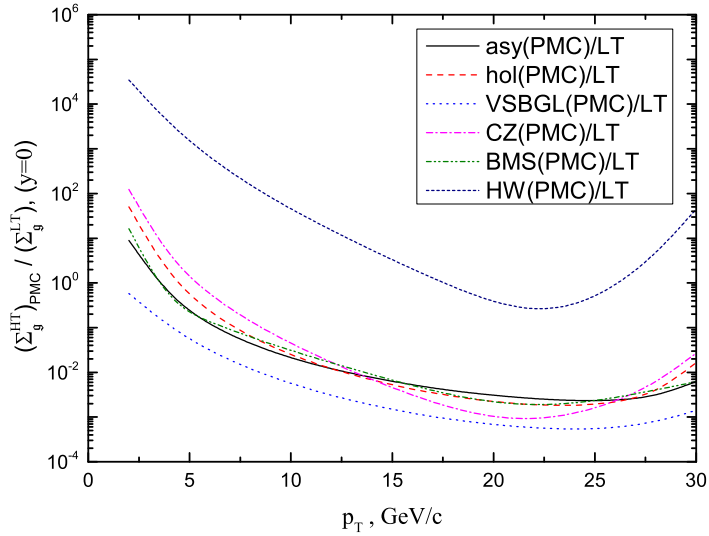


FIG. 8: Ratio $(\Sigma_g^{HT})_{PMC}/(\Sigma_g^{LT})$, in the process $\pi^+ p \rightarrow gX$, as a function of the p_T of the gluon at $\sqrt{s} = 62.4 \text{ GeV}$.

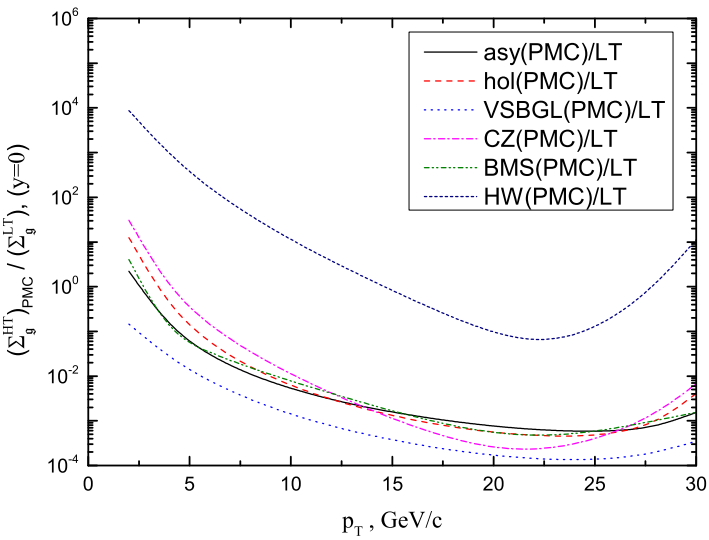


FIG. 9: Ratio $(\Sigma_g^{HT})_{PMC}/(\Sigma_g^{LT})$, in the process $\pi^- p \rightarrow gX$, as a function of the p_T of the gluon at $\sqrt{s} = 62.4 \text{ GeV}$.

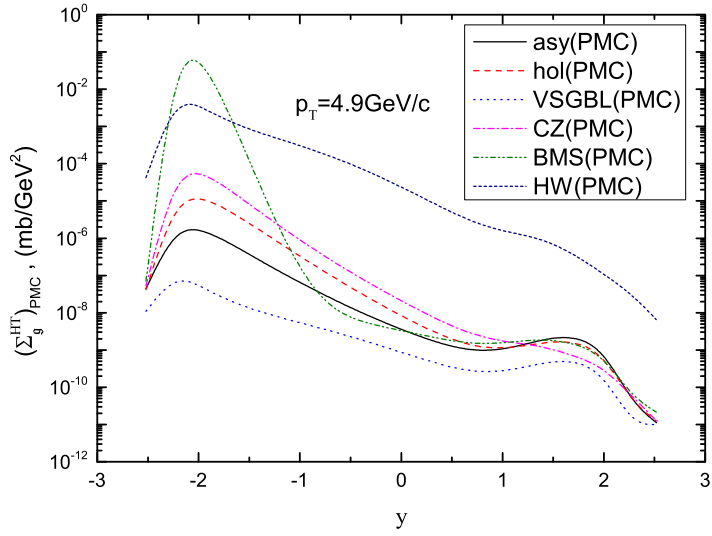


FIG. 10: Higher-twist $\pi^+ p \rightarrow gX$ inclusive gluon production cross section $(\Sigma_g^{HT})_{PMC}$, as a function of the y rapidity of the gluon at $p_T = 4.9 \text{ GeV}/c$, at $\sqrt{s} = 62.4 \text{ GeV}$.

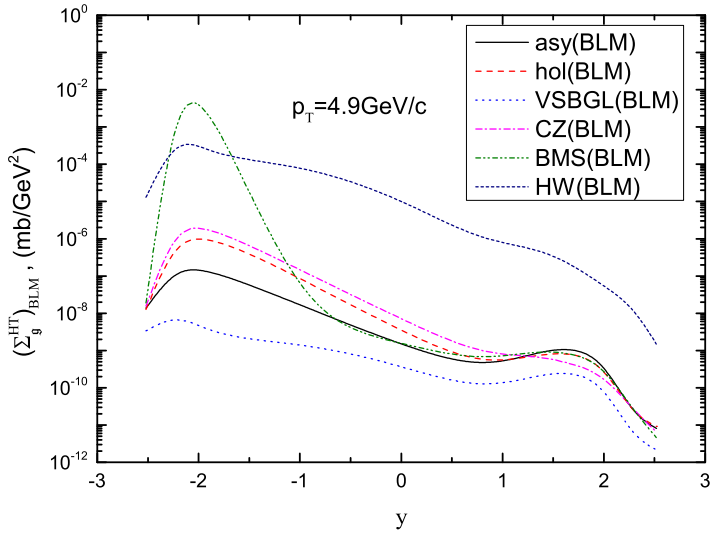


FIG. 11: Higher-twist $\pi^+ p \rightarrow gX$ inclusive gluon production cross section $(\Sigma_g^{HT})_{BLM}$, as a function of the y rapidity of the gluon at $p_T = 4.9 \text{ GeV}/c$, at $\sqrt{s} = 62.4 \text{ GeV}$.

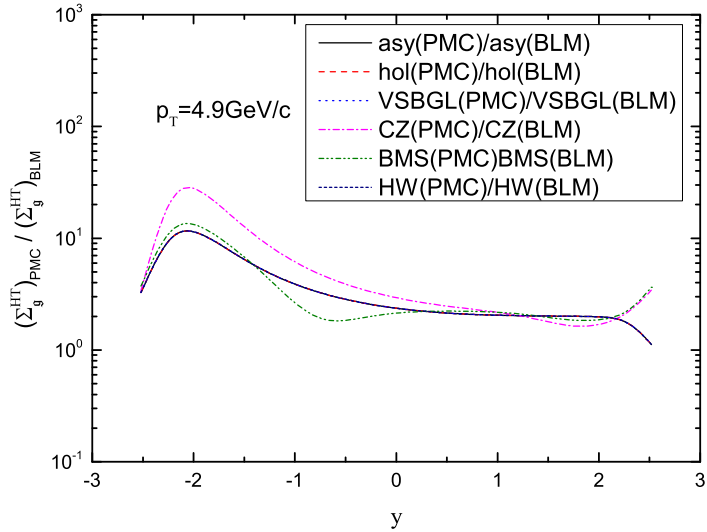


FIG. 12: Ratio $(\Sigma_g^{HT})_{PMC}/(\Sigma_g^{HT})_{BLM}$, in the process $\pi^+p \rightarrow gX$, as a function of the y rapidity of the gluon at $p_T = 4.9 \text{ GeV}/c$, at $\sqrt{s} = 62.4 \text{ GeV}$. Notice that curves for asy(PMC)/asy(BLM), hol(PMC)/hol(BLM), VSBGL(PMC)/VSBGL(BLM), HW(PMC)/HW(BLM) pion distribution amplitudes completely overlap.

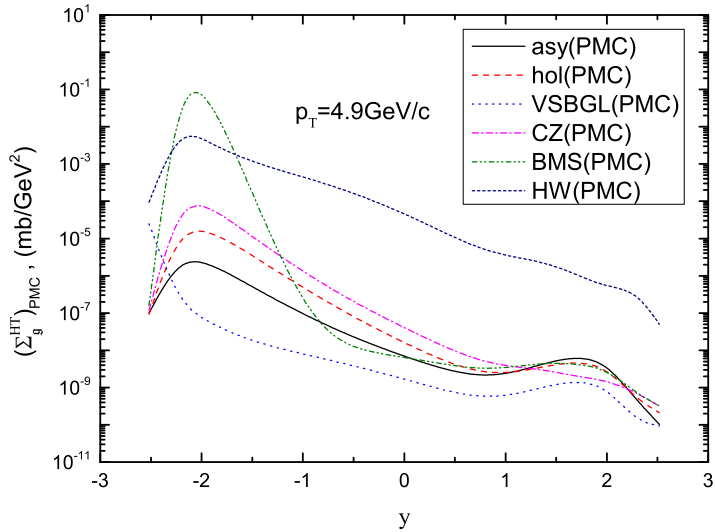


FIG. 13: Higher-twist $\pi^-p \rightarrow gX$ inclusive gluon production cross section $(\Sigma_g^{HT})_{PMC}$, as a function of the y rapidity of the gluon at $p_T = 4.9 \text{ GeV}/c$, at $\sqrt{s} = 62.4 \text{ GeV}$.

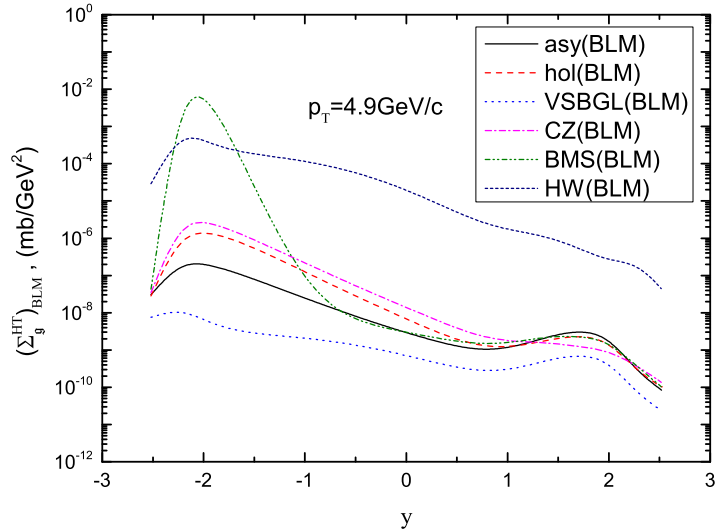


FIG. 14: Higher-twist $\pi^- p \rightarrow gX$ inclusive gluon production cross section $(\Sigma_g^{HT})_{BLM}$, as a function of the y rapidity of the gluon at $p_T = 4.9 \text{ GeV}/c$, at $\sqrt{s} = 62.4 \text{ GeV}$.

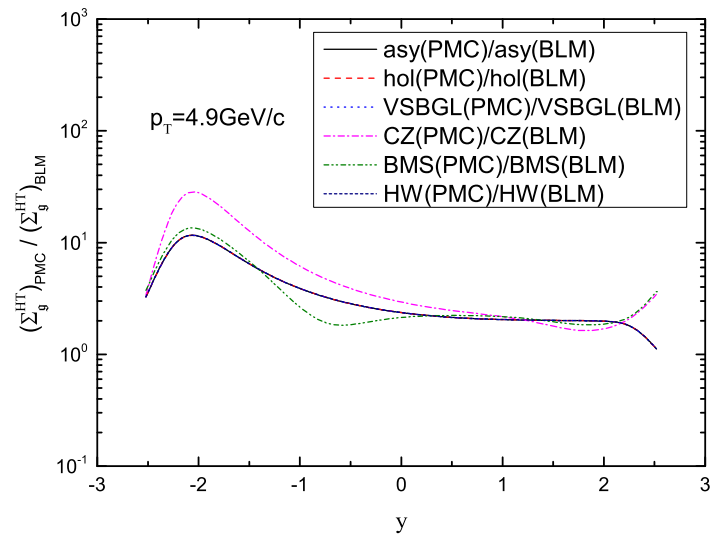


FIG. 15: Ratio $(\Sigma_g^{HT})_{PMC} / (\Sigma_g^{HT})_{BLM}$, in the process $\pi^- p \rightarrow gX$, as a function of the y rapidity of the gluon at $p_T = 4.9 \text{ GeV}/c$, at $\sqrt{s} = 62.4 \text{ GeV}$. Notice that curves for asy(PMC)/asy(BLM), hol(PMC)/hol(BLM), VSBGL(PMC)/VSBGL(BLM), HW(PMC)/HW(BLM) pion distribution amplitudes completely overlap.